INTERFACE

rsif.royalsocietypublishing.org

Research

Cite this article: Goyens J, Van Wassenbergh S, Dirckx J, Aerts P. 2015 Cost of flight and the evolution of stag beetle weaponry. *J. R. Soc. Interface* **12**: 20150222.
http://dx.doi.org/10.1098/rsif.2015.0222

Received: 12 March 2015
Accepted: 26 March 2015

Subject Areas:
biomechanics

Keywords:
sexual selection, mandible, stag beetle, Lucanidae, cost of flight, computational fluid dynamics

Author for correspondence:
Jana Goyens
e-mail: jana.goyens@uantwerpen.be

Cost of flight and the evolution of stag beetle weaponry

Jana Goyens[1,2], Sam Van Wassenbergh[1,3], Joris Dirckx[2] and Peter Aerts[1,4]

[1]Laboratory of Functional Morphology, University of Antwerp, Universiteitsplein 1, 2610 Antwerp, Belgium
[2]Laboratory of Biophysics and BioMedical Physics, University of Antwerp, Groenenborgerlaan 171, 2020 Antwerp, Belgium
[3]Department of Biology, Ghent University, K.L. Ledeganckstraat 35, 9000 Ghent, Belgium
[4]Department of Movement and Sport Sciences, Ghent University, Watersportlaan 2, 9000 Ghent, Belgium

Male stag beetles have evolved extremely large mandibles in a wide range of extraordinary shapes. These mandibles function as weaponry in pugnacious fights for females. The robust mandibles of *Cyclommatus metallifer* are as long as their own body and their enlarged head houses massive, hypertrophied musculature. Owing to this disproportional weaponry, trade-offs exist with terrestrial locomotion: running is unstable and approximately 40% more costly. Therefore, flying is most probably essential to cover larger distances towards females and nesting sites. We hypothesized that weight, size and shape of the weaponry will affect flight performance. Our computational fluid dynamics simulations of steady-state models (without membrane wings) reveal that male stag beetles must deliver 26% more mechanical work to fly with their heavy weaponry. This extra work is almost entirely required to carry the additional weight of the massive armature. The size and shape of the mandibles have only negligible influence on flight performance (less than 0.1%). This indicates that the evolution of stag beetle weaponry is constrained by its excessive weight, not by the size or shape of the mandibles and head as such. This most probably paved the way for the wide diversity of extraordinary mandible morphologies that characterize the stag beetle family.

1. Introduction

In sexual selection theory, the differential costs of sexual traits are essential to balance their benefits and to ensure honest signalling. However, it has been hard to prove these costs experimentally [1,2]. Even in species with very impressive ornaments and armaments, the costs are often relatively small. For example, peacock trains (6.9% of body mass) do not decrease take-off performance, and rhinoceros beetle horns (1.5% of body mass) do not influence flight distance, travel speed or aerodynamic costs [3–5]. The detection of such costs is even harder when animals have also evolved compensatory traits [2]. For example, malachite sunbirds have increased their wingspan to compensate for the negative effects of their long tail (0.3% of body mass) on flight cost and manoeuvrability [6], and swordtail fishes have a larger heart ventricle to compensate for the decreased swimming endurance because of their long tail [7]. The costs of bearing weapons become more evident when the armaments are heavier. Walking around with hermit crab chelipeds (30% of body mass), fiddler crab claws (50% of body mass) or stag beetle mandibles and their musculature (18% of body mass) is energetically very costly [8–10]. Stag beetle males need their robust mandibles and the associated massive muscles to bite extremely forcefully (three times as forcefully as scaled female bites) in their aggressive battles [11] (figure 1). As a result, the heavy armature not only increases the energy cost of running, but *Cyclommatus metallifer* stag beetles are also statically unstable twice every stride [10]. Therefore, flying is most probably essential to cover larger distances towards females and nesting sites. The importance of flight over running has also been observed for the European *Lucanus cervus* stag beetles [12]. It should therefore be questioned whether or

THE ROYAL SOCIETY PUBLISHING

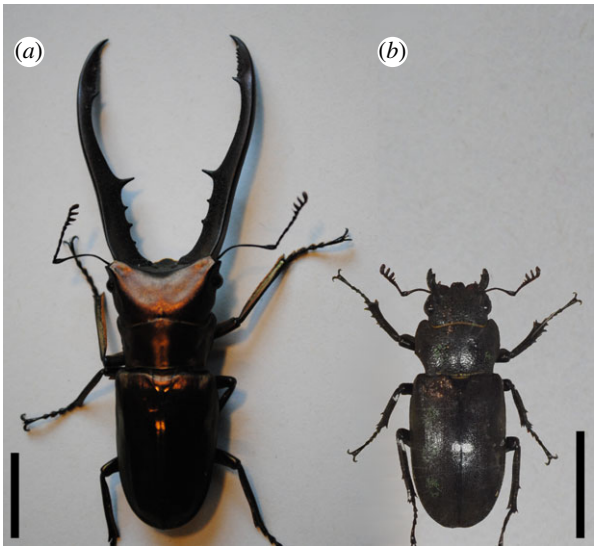

Figure 1. Photos of a male (*a*) and a female (*b*) *Cyclommatus metallifer*, scaled to equal abdomen plus meta- and mesothorax length. Scale bars indicate 1 cm. (Online version in colour.)

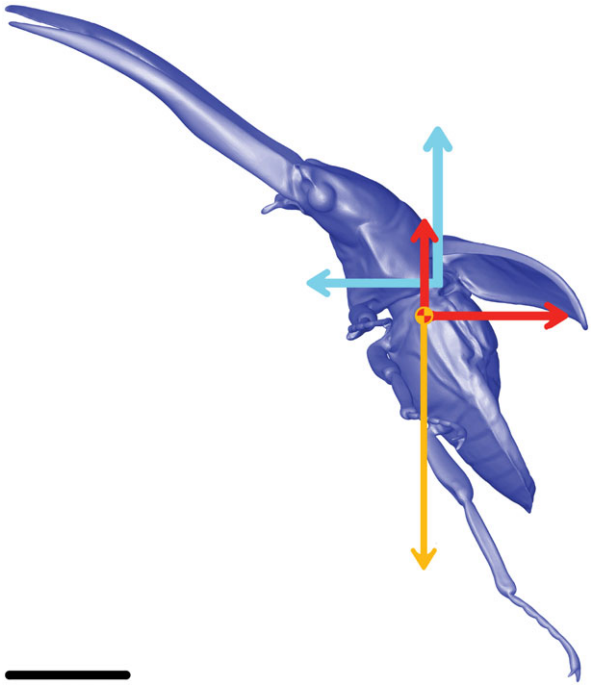

Figure 2. Schematic overview of the forces acting upon the flying stag beetle. Orange: body centre of mass and gravitational force. Red: aerodynamic forces (drag and lift) that are provided by CFD simulations. Blue: calculated wing forces (thrust and lift) that must be produced by the wings in order to maintain a steady, horizontal flight. The scale bar indicates 1 cm, the vector lengths have only illustrative purposes.

not the weaponry impairs the aerial performance of male stag beetles. If so, this would be an important factor in the evolution of stag beetle armature.

In this paper, we investigate the influence of stag beetle weaponry on their cost of flight, by simulating the aerodynamic forces and moments on a flying stag beetle body with computational fluid dynamics (CFD). Given the high armature mass, we hypothesize that the associated increase in the cost of flight will be significant, as opposed to that of the lightweight horns of rhinoceros beetles. In addition to calculating the effect of the weight of the armature, we will quantify the energetic and aerodynamic consequences of its size and shape, as these characteristics determine the flow of air around the head during flight. Armature weight, size and shape are obviously inter-related. Theoretically, however, these aspects can be decoupled from each other in the case of structural changes (e.g. cuticle thickness). Size and shape (and not the weight as such) determine the aerodynamic performance of the morphology. Therefore, from an evolutionary point of view, it is important to consider the effects of armature size and shape on the net mechanical flight cost separately. We therefore test the aerodynamic and energetic consequences of different mandible weights, sizes and shapes explicitly, by comparing CFD models with modified armature.

2. Material and methods

2.1. Micro-computed tomography imaging

We obtained *C. metallifer* stag beetles from a commercial dealer (Kingdom of Beetle, Taipei, Taiwan). The anterior body part of the male and female specimens was scanned by the Centre for X-ray Tomography of Ghent University (voxel sizes of, respectively, 38 µm and 13 µm). For the posterior body parts, we used the Skyscan 1172 high-resolution micro-CT scanner (Bruker micro-CT, Kontich, Belgium; voxel size of 13 µm for both the male and the female specimens). The same Skyscan micro-CT scanner was used for the limbs (voxel size of 27 µm for both sexes), and the mandibles of four other stag beetle species (voxel size of 13 µm for *Lamprima adolphinae*, *Dorcus bucephalus* and *Prismognathus davidis*; 11 µm for *Nigidius obesus*).

2.2. Three-dimensional beetle model

Using the micro-CT scans, we created surface models of each of the body parts (head, thorax, abdomen, mandibles, limbs, elytra). This was performed in the three-dimensional image processing software Amira (v. 5.4.4; VSG Systems, Mérignac, France), in which we annotated the voxels that belong to the body using automatic thresholds (based on greyscale values) and manual corrections in the three orthogonal views. To obtain information on the natural flight position, we made video recordings (125 frames s^{-1}, JVC GZ-V515; JVC Kenwood Corporation, Kanagawa, Japan) of flying male stag beetles in the laboratory. We positioned the triangulated three-dimensional surface models of the body parts relative to each other and the global frame of reference (Capture v. 11; Geomagic, Cary, NC; figure 2). The hard wing covers (elytra) of dead specimens were manipulated to find their 'locked position' as adopted in flight [13,14]. The entire beetle body, yet without the membrane wings, was represented as one single rigid body for which force and moment balances were calculated (similar to the approach of Taylor & Thomas [15] for the desert locust and Sum & Xiong [16] for the bumblebee). As we consider only the body in our simulations, the aerodynamic interactions between the body and the membrane wings are neglected. For example, interactions of the flapping wings with vortices that are shed by the body are not considered. However, because numerical Navier–Stokes simulations have shown that the aerodynamic interactions between the body and the wings of insects are negligible, their aerodynamic characteristics can adequately be analysed separately [17]. By performing CFD simulations (see below), the net forces (i.e. as averaged over a wing beat cycle) and therefore also the external work (i.e. whole body level) per unit distance that need to be delivered by the wings can be calculated. This

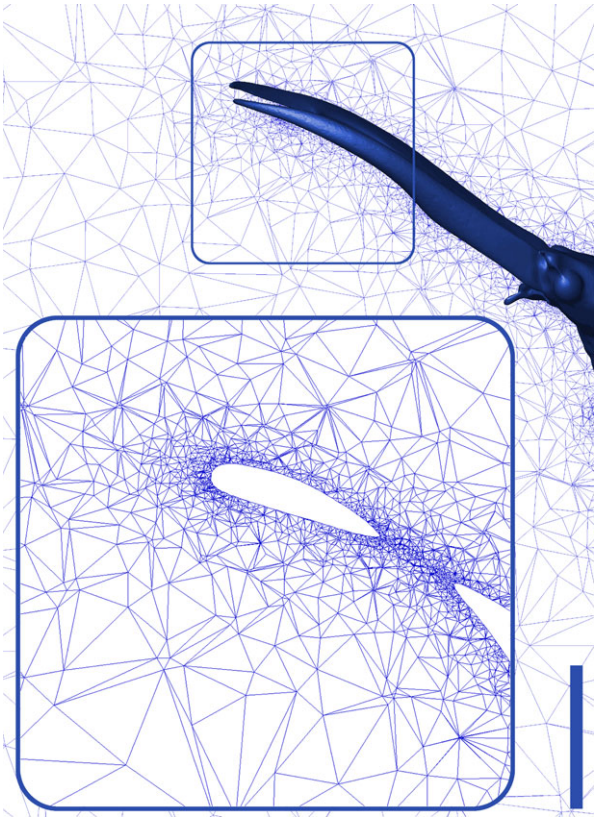

Figure 3. Sagittal section of the CFD mesh. The closer to the beetle model, the smaller the mesh elements are. The inset shows an enlargement of the mesh elements near the distal half of the mandibles. The scale bar indicates 1 cm. (Online version in colour.)

enables the straightforward comparisons of the effect of the mandibles aimed at in this paper.

2.3. Computational fluid dynamic simulations

We constructed a virtual wind tunnel around the beetle model in DESIGNMODELLER (v. 14.5; Ansys, Canonsburg, PA). The boundaries of the virtual wind tunnel left sufficient space around this rigid body to prevent artefacts. The volume between these boundaries and the beetle model was subsequently filled with tetrahedrons. To enhance the accuracy, this mesh became finer the closer it was to the beetle model (figure 3). The required number of mesh elements were tested in a convergence analysis (see below).

In FLUENT (v. 14.5; Ansys, Canonsburg, PA), a velocity inlet was created in the boundary in front of the beetle model, with a horizontal flow directed towards the anterior side of the stag beetle model. The velocity was $0.57\,\mathrm{m\,s^{-1}}$, corresponding to the highest flight velocity observed. The boundaries that are parallel with the flow direction were modelled as moving walls with the same velocity as the air. A pressure outlet was defined at the exit of the virtual wind tunnel.

The Reynolds number (*Re*) is

$$Re = \frac{\rho v L}{\mu} = \frac{1.2\,\mathrm{kg\,m^{-3}} \times 0.57\,\mathrm{m\,s^{-1}} \times 0.032\,\mathrm{m}}{1.82 \times 10^{-5}\,\mathrm{Pa\,s}} = 1203,$$

where ρ is the density of air at 20°C, v is the flow velocity, L is the length of the beetle along the flow direction and μ is the dynamic viscosity of air at 20°C. Based on this intermediate *Re*, we assumed a laminar boundary layer, although the wake may already show turbulent flow patterns [18]. Therefore, a transition shear-stress transport flow model was used [19]. The Reynolds-averaged equations of a fluid flow were solved numerically through the finite-volume method. We used a node-based Green–Gauss gradient treatment, because it achieves higher accuracy than cell-based gradient treatments in unstructured tetrahedral meshes (Ansys user manual). The simulations ran until convergence of the scaled flow equation residuals was reached, usually after approximately 3000 iterations. The total drag and lift forces on the rigid body were computed by FLUENT. These forces apply at the body centre of mass, are directed, respectively, horizontally and vertically and take both pressure and viscous force components into account.

2.4. Convergence analysis

The number of tetrahedral mesh elements in our simulation is a compromise between computational power and accuracy. We compared the aerodynamic forces and moments of 28 models of between 300 000 and 10 million mesh elements. For the mesh with 2.7 million elements, used for the simulation experiments, the relative aerodynamic differences with the finest mesh model output was only 2.2%.

2.5. Validation

We simulated a sphere with the *Re* of the beetle under the same settings as the beetle simulations. The simulation predicted a drag coefficient of 0.49, which is nearly identical to the experimentally determined value of 0.47 [20]. Furthermore, a recent study using almost identical model settings proved accurate in calculating the forces and moments by the flow around the more complex biological shapes of boxfish carapaces [21].

2.6. Force balance

The CFD simulations provide the aerodynamic forces and moments that apply on the steadily and horizontally flying rigid body. The gravitational force acts at its centre of mass. The equilibrating external forces and moments needed to maintain this steady state can derive only from the wings and must be considered as the net effect (in terms of forces and moment transfer) from the wings to the body as averaged over a wing beat cycle. These net forces and moments apply on the rigid body almost vertically above the experimentally determined position of the body centre of mass [10]. Horizontal and vertical forces (wing, aerodynamic and gravity) must cancel each other out to proceed in a steady horizontal manner (figure 2). Note that the moments of the forces (wing and aerodynamic), as well as potential direct torque transfer from the wings on the body, must be in equilibrium to maintain the average orientation of the body over a cycle. The moment balance is, however, redundant for the present analysis, hence it is not considered further. The cycle-averaged wing forces derive from the net work done by the flight muscles. As such, these forces can be considered a direct measure for the *net mechanical energy requirements per unit distance covered* (net mechanical cost of flight). It should be noted that the present simulations pretend by no means to reflect the instantaneous unsteady features of the dynamics of insect flight. These simulations deliberately aim at capturing just the basic costs of the beetle's flight (void of all intricate confounding factors) useful for a solid comparison.

2.7. Simulation experiments

We compared the complete beetle model with other models to assess the influence of the mandible's weight, size and shape on the aerodynamic and wing forces:

— *Weight*: *complete* model versus a model *without mandibles* and a model of a *non-dimorph* conspecific. The *non-dimorph* state is represented by the scaled female morphology, because the male and female morphology is very alike in stag beetle species without sexual dimorphism [10,22] (figures 1 and 4*a*,*c*,*d*).

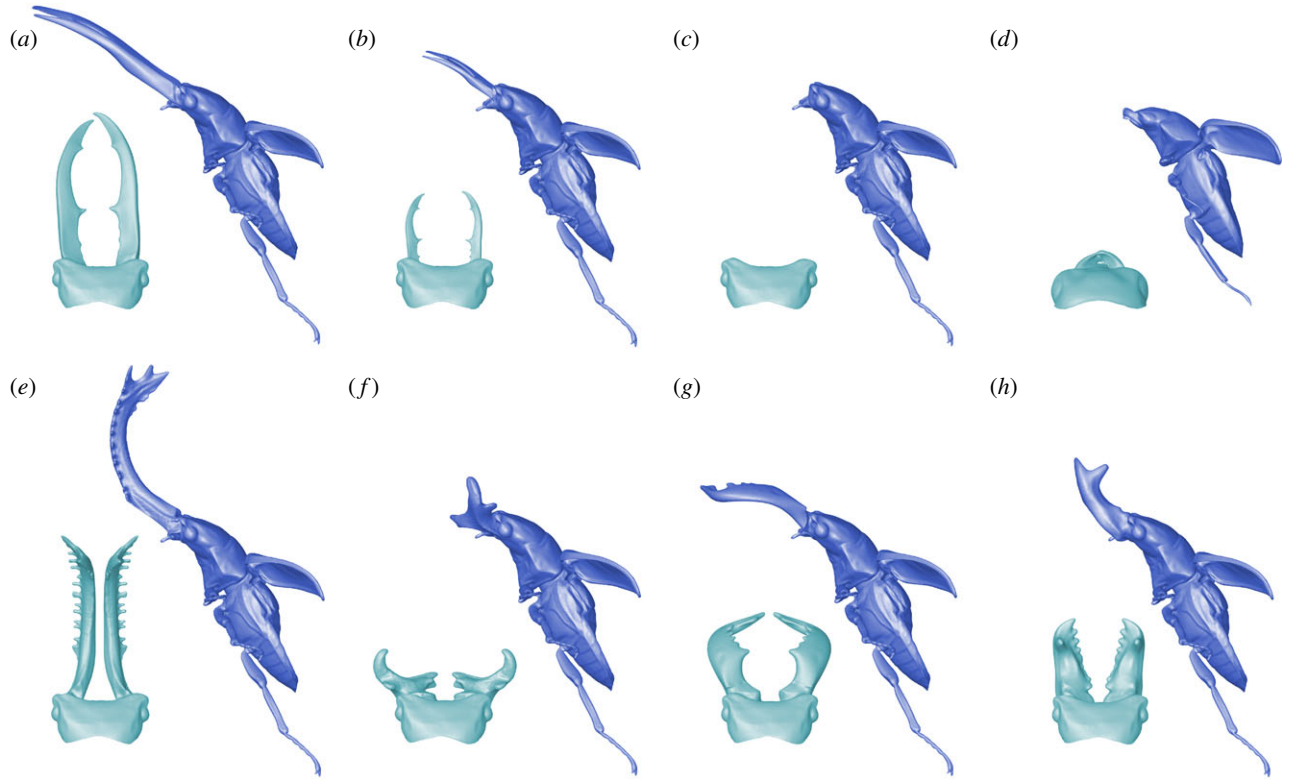

Figure 4. Geometric three-dimensional models of stag beetle bodies and heads. The beetle bodies are shown in dark blue in the lateral view; the heads in light blue in the dorsal view. (*a*) *Complete* model; (*b*) *short mandibles* model; (*c*) *without mandibles* model; (*d*) *non-dimorph* model; (*e*) model with mandibles of *Lamprima adolphinae*; (*f*) model with mandibles of *Nigidius obesus*; (*g*) model with mandibles of *Dorcus bucephalus*; (*h*) model with mandibles of *Prismognathus davidis*. (Online version in colour.)

Table 1. Average mass (g) and standard deviation for 10 males and 10 females and the male that was used to build the model. MMA, posterior body part (meso- and metathorax and abdomen, without legs); HP, anterior body part (head and prothorax, including mandibles, without legs).

	male in model	male ($n = 10$)	female ($n = 10$)
total mass	1.34	1.21 ± 0.27	0.33 ± 0.12
MMA mass	0.70	0.65 ± 0.14	0.218 ± 0.079
HP mass	0.54	0.46 ± 0.15	0.082 ± 0.032
mandible mass	0.12		

The *non-dimorph* model was scaled in such a way that the posterior body part (meso- and metathorax + abdomen) was as large as in the *complete* model [10]. For both the *without mandibles* and *non-dimorph* model, the total mass was reduced to conform to our weight measurements (on fresh material with an analytical microbalance; MT5; Mettler Toledo, Columbus, OH; precision: 5 µg; table 1), and the position of the centre of mass was adapted according to the altered model volume. The differences in the aerodynamic forces between the *complete* model and the two other models reveal the influence on the aerodynamic drag and lift of the large mandibles (for the *without mandibles* model) or the large mandibles and bite muscles (for the *non-dimorph* model).

— *Size*: *complete* model versus a model with *short mandibles* (isometrically scaled to half the original length; figure 4*b*) and the model *without mandibles* (i.e. infinitely small mandibles). Because we want to examine the size effect separately from the weight effect, we simulated these three models with an identical total body mass and position of the body centre of mass. Hence, the *without mandibles* model in the size comparison differs from the *without mandibles* model in the weight comparison. In nature, the male mandible size varies strongly between *C. metallifer* individuals [23]. We use isometrically scaled mandibles for the *short mandibles* model, to exclude the additional shape effects that would have occurred if we would have used the naturally short mandibles of a conspecific individual.

— *Shape: complete* model versus four models with mandibles of different stag beetle species (figure 4*e–h*). In these models, we replaced the original mandibles with those of other species (*L. adolphinae*, *N. obesus*, *Dorcus bucephalus*, *P. davidis*; figure 4*e–h*). We scaled the mandibles to the same cuticle volume as the original mandibles, to arrive at a similar armature weight (i.e. assuming the same mass density of the mandible cuticle). We used armature weight as a scaling factor, rather than the frontal surface area, because the latter already partly eliminates the shape effect. All models in the shape comparison had the same body mass and location of the body centre of mass as the *complete model*, in order to exclude the weight effects.

We calculated the frontal area of the models, which is defined as the projected area of the beetle (at the body angle of attack used in the model) on a plane perpendicular to the flow direction. Combining this frontal area (A) with the drag force (F_D, as calculated by CFD), we calculated the coefficient of drag (C_D) of the entire beetle body using the formula of aerodynamic drag: $F_D = 1/2\ C_D\ \rho v^2 A$. To arrive at coefficients of drag of the mandibles only, we subtracted the drag force and frontal area of the models *without* mandibles from those of the model *with* mandibles.

3. Results

The mandibles of the male *C. metallifer* individual that was used to build the model weighed 8.7% of its body mass

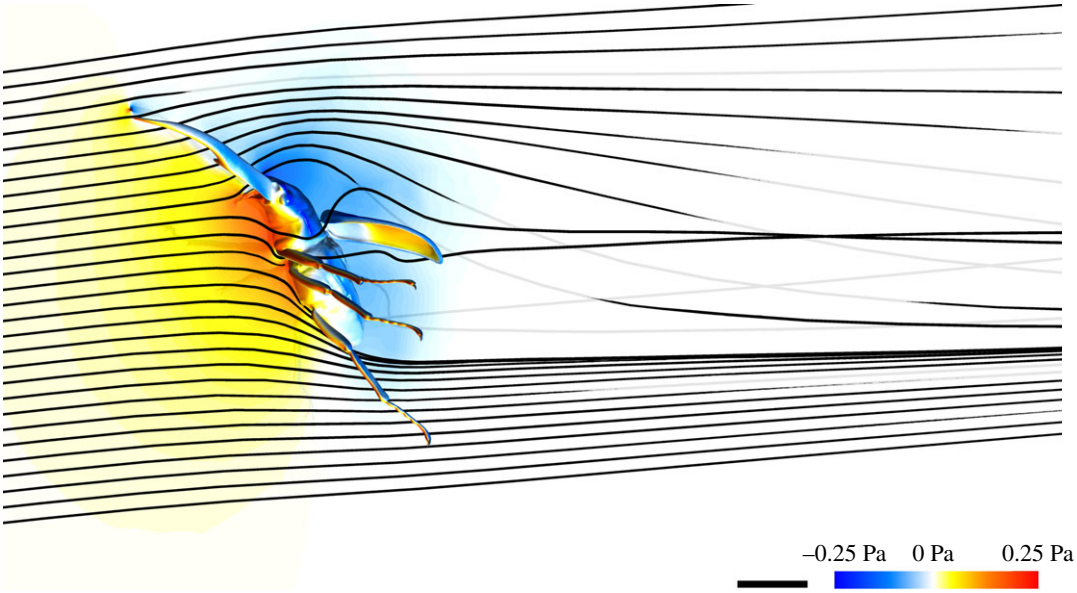

Figure 5. Streamlines and pressure. The pressure on the stag beetle body and the air pressure (relative to ambient static pressure) in the mid-sagittal plane are shown. Black lines indicate streamlines starting at 30 evenly distributed points on the mid-sagittal plane in front of the beetle. The scale bar indicates 1 cm.

(table 1). The complete sexual dimorphism of its head (taking the scaled weight of the female head into account), weighed 23% of its body mass (table 1). This is close to the value that we calculated for a population of 10 male individuals (18%; table 1). Male *C. metallifer* stag beetles fly at a body angle of 58° (±14° s.d.). We recorded a maximal velocity of 0.57 m s^{-1} (on average 0.46 m s^{-1} ± 0.13 m s^{-1} s.d.) which is relatively slow compared with similarly sized rhinoceros beetles [3,4]. We implemented these characteristics in a CFD model, to calculate the aerodynamic forces and moments on a steadily and horizontally flying male stag beetle body (without the wings).

The simulations show how air flows over and around the body and the mandibles (figures 5 and 6). The flow separates approximately when passing the widest points on both sides of the mandibles, causing a wide low-pressure region behind the mandibles. The same is true for the rest of the body. Hence, both are poorly streamlined and the beetle has a high C_D (table 2). This causes a high (pressure) drag force on the beetle. Averaged over a wing beat cycle, the summed effects of the aerodynamic and gravitational forces on the body must be balanced by thrust and lift that are produced by the wings (figure 2).

3.1. Weaponry weight

The gravitational force (1.3×10^{-2} N) is several orders of magnitude larger than the aerodynamic forces on the stag beetle body (1.2×10^{-4} N drag and 6.1×10^{-5} N lift; table 2). This suggests that the weight of the heavy weaponry (mandibles + head) has a significant impact on the required membrane wing forces, hence also on the net work done by the flight muscles. As such, the membrane wing forces can be considered a direct measure for the net mechanical energy requirements per unit distance covered (net mechanical cost of flight). We evaluate this weight effect by comparing the results of the CFD simulations of the *complete* three-dimensional beetle model (figure 4*a*), a model that lacks the mandibles (*without mandibles* model; figure 4*c*), and a model of a non-dimorph conspecific (size-normalized *non-dimorph* model; figure 4*d*).

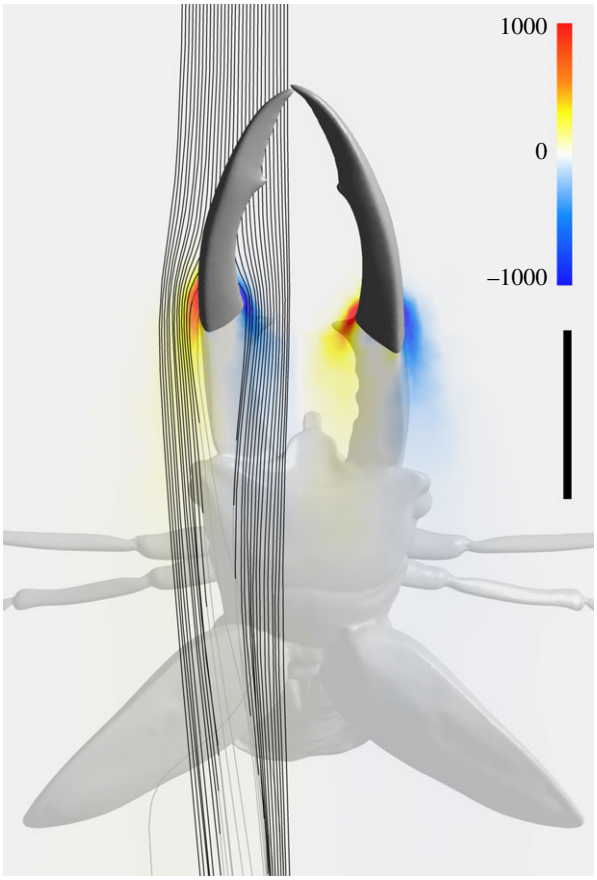

Figure 6. Streamlines and vorticity. Black lines indicate streamlines starting at 30 evenly distributed points on a horizontal line in front of the beetle. The vorticity (Hz) around the vertical axis is shown in a horizontal plane. Positive values (shown in red) indicate counter-clockwise vorticity, negative values (shown in blue) indicate clockwise vorticity. High vorticity is observed in the boundary layer of the flow-facing side of the mandible to continue downstream of the separation point. The scale bar indicates 1 cm.

The differences in the aerodynamic forces between the *complete* model and the two additional models can be attributed to the sexual dimorphism (mandibles and, in the case of the *non-dimorph* model, the accompanying muscles). The mandibles

Table 2. Aerodynamic and wing forces. Forces are provided for the *complete* model and the models of the shape, size and weight comparisons. For the shape comparison, letters indicate the origin of the mandibles: (La) *Lamprima adolphinae*; (Ni) *Nigidius obesus*; (Do) *Dorcus bucephalus*; (Pr) *Prismognathus davidis*. The percentages give the relative difference from the '*complete*' model; negative values indicate that the model has a lower force than the '*complete*' model. C_D, coefficient of drag; *L/D*, lift to drag ratio; NMFC, net mechanical flight cost (as represented by the wing force; see text).

		weight		size		shape			
	complete	*without mandibles*	*non-dimorph*	*short mandibles*	*without mandibles*	La	Ni	Do	Pr
frontal area (cm^2)	5.61	4.98	3.38	5.11	4.98	6.17	5.30	5.45	5.61
$C_{D,body}$	1.04	1.04	0.99	1.06	1.04	1.10	1.04	1.05	1.04
$C_{D,mandibles}$	1.03			1.57		1.31	1.06	1.15	1.01
drag (10^{-4} N)	−1.2	−1.1	−0.70	−1.1	−1.1	−1.4	−1.2	−1.2	−1.2
lift (10^{-4} N)	0.61	0.50	0.337	0.54	0.50	0.52	0.55	0.59	0.57
L/D	−0.50	−0.46	−0.48	−0.48	−0.46	−0.37	−0.47	−0.49	−0.47
drag difference (%)		−12%	−43%	−7.6%	−11%	16%	−5.3%	−1.9%	0.3%
lift difference (%)		−18%	−45%	−12%	−18%	−14%	−10%	−3.2%	−6.5%
NMFC (N)	0.013	0.012	0.010	0.013	0.013	0.013	0.013	0.013	0.013
NMFC difference (%)		−8.4%	−26%	0.055%	0.081%	0.068%	0.047%	0.015%	0.030%

create some lift, but have a negative effect on drag. The same is true for the wide male head (table 2). The mandibles (11% of body weight) have a pronounced negative effect on the mechanical cost of flight (8.4% more costly than the *without mandibles* model). When we also take the effect of the enlarged head into account (in total 27% of body weight, compared with the *non-dimorph* model), the mechanical cost of the sexual dimorphism increases to 26%.

3.2. Weaponry size

To investigate the pure size effect of the mandibles, we compare three geometrically different models (figure 4*a–c*; *complete*, *short mandibles* and *without mandibles*), yet with an identical total body mass. The *complete* model experiences more lift, but also more drag, than the *short mandibles* model. We find a similar, but more pronounced, difference when using the *without mandibles* model that mimics infinitely small mandibles (table 2). However, the aerodynamic changes owing to the altered mandible size do not affect the net mechanical flight cost at all (less than 0.1% difference from the *complete* model; table 2).

3.3. Weaponry shape

To assess the influence of the shape or 'ornamentation' of the weaponry, we use four additional models in which the original mandibles are replaced by those of other stag beetle species (figure 4*e–h*). By scaling the mandibles in such a way that cuticle volume remains identical, we exclude weight differences. The mandible shape influences the aerodynamic forces. For example, the large and ornamented mandibles of *Lamprima adolphinae* cause a high frontal area and C_D (table 2). Hence, the model experiences more drag, and, combined with a decreased lift force, this results in the lowest absolute lift-to-drag ratio magnitude of all models (0.37; table 2). However, it is clear that the shape effect is trivial compared with the weight effect of the weaponry and its musculature (less than 0.1% difference from the *complete* model; table 2).

4. Discussion

4.1. Performance consequences of weaponry weight

In many species, elaborate ornaments and armaments incur no, or only subtle, costs [1]. This is, for example, the case for flying with rhinoceros horns (1.5% of body weight), hummingbird tails (0.4% of body weight) and peacock trains (6.9% of body weight) [3,5,24]. Species for which substantial costs of ornaments were observed often compensate for these costs, for example, by increasing power generation with a larger wingspan (e.g. sunbird tails, 0.3% of body weight; earwig forceps) and/or flight muscles (e.g. stalk-eyed flies, 4.92% of body weight) [2,6,25]. Stag beetle mandibles are more extreme in terms of armament weight. Because fighting males must bite forcefully, they have not only robust mandibles but also a massive head to house the large bite muscles [11,26]. In *Lucanus maculifemoratus* [27] and *C. metallifer* stag beetles, this results in a head that weighs, respectively, 28% and 18% of the total male body weight. Moreover, nutritional constraints cause stag beetles with large mandibles to develop relatively small wings [28]. Therefore, they do not compensate for the flight cost of their heavy armature by an increased wing span. Consequently, our CFD models highlight an evolutionary constraint: *natural* selection on flight cost hampers the *sexual* selection towards heavier armaments in male stag beetles. This is in addition to the negative effect of armature weight on the cost and stability of male terrestrial locomotion [10].

4.2. Evolution of weaponry size and shape

The size and shape of stag beetle weaponry determine the dynamics of the air flow over the flying beetle body. None of the models show signs of a delayed flow separation at any position along their mandibles, and all models have large coefficients of drag ($C_D > 1$; table 2). These C_Ds are comparable to those of an upright cyclist or a circular cylinder (with its axis normal to the flow at a *Re* of about 10^3) [18,20]. Hence, the mandibles are poorly streamlined. However, the aerodynamic forces are very small compared with the gravitational force. This relative difference depends on the flight velocity, but, even if the beetles flew a lot faster, the conclusions would still hold true: at a hypothetical forward velocity of 2 m s^{-1} (3.5 times as fast as in reality), the maximal effect of size and shape would only be 1%. Hence, the aerodynamic effects of the weaponry size and shape are swamped by the weight effect. Therefore, the strong sexual selection for large mandibles and bite muscles has (contra-intuitively) released the constraints on mandible sizes and shapes. Consequently, the absence of a selective pressure to enhance the lift properties and to streamline the mandibles probably provided the freedom to evolve the wide variety of elaborate mandible morphologies that is characteristic for the stag beetle family Lucanidae [29] (figure 4*e–h*). Also for other animal taxa (e.g. rhinoceros horns and avian tails), it was argued that the low cost of these armaments/ornaments causes their remarkable diversification owing to more labile evolution [3,24]. However, the origin of the low armament/ornament cost differs: the selective pressure on stag beetle mandible morphology is minimal because of the dominant effect of weight on the net flight cost, whereas for rhinoceros horns and avian tails this is the case because of a relative large wake from the body compared with the armament/ornament [3,24].

5. Conclusion

We used flow simulations to compare the effects of weaponry weight, size and shape on the net additional wing force that male stag beetles have to deliver in order to maintain a steady, horizontal flight. Even though these three characteristics are intuitively inter-related (e.g. larger structures are often heavier), they can change independently in case of structural changes (e.g. a larger structure with a thinner cuticle). The weight of the armament determines the gravitational force, and its size and shape determine the aerodynamic forces. We showed that, because of the robust mandibles and their hypertrophied muscles, stag beetle flight is heavily dependent on armature weight. Relative to this weight effect, the impact of armature size and shape is negligible. Such a decoupling between morphology (size, shape) and weight of armaments and ornaments may well be a more general characteristic of flying animals. This was for example suggested, but not explicitly tested, for rhinoceros beetles [30]. For the stag beetle family, the low cost of the weaponry morphology probably made it liable to evolutionary changes, which led to its extraordinary diversity in mandible sizes and shapes.

Acknowledgements. The authors thank Ms Josie Meaney for proofreading of the manuscript.

Funding statement. This study was supported by a BOF grant (ID BOF UA 2011-445-a) of the Research Council of the University of Antwerp. The micro-CT reconstructions of the anterior body parts were provided by the Centre for X-Ray Tomography, Ghent University, Belgium. The Sky-Scan 1172 high-resolution micro-CT scanner, located at the VUB facilities, was funded by the Hercules Foundation (grant no. UABR/ 11/004).

References

1. Kotiaho JS. 2001 Costs of sexual traits: a mismatch between theoretical considerations and empirical evidence. *Biol. Rev.* **76**, 365–376. (doi:10.1017/S1464793101005711)
2. Husak J, Swallow J. 2011 Compensatory traits and the evolution of male ornaments. *Behaviour* **148**, 1–29. (doi:10.1163/000579510X541265)
3. McCullough EL, Tobalske BW. 2013 Elaborate horns in a giant rhinoceros beetle incur negligible aerodynamic costs. *Proc. R. Soc. B* **280**, 20130197. (doi:10.1098/rspb.2013.0197)
4. McCullough EL, Weingarden PR, Emlen DJ. 2012 Costs of elaborate weapons in a rhinoceros beetle: how difficult is it to fly with a big horn? *Behav. Ecol.* **23**, 1042–1048. (doi:10.1093/beheco/ars069)
5. Askew GN. 2014 The elaborate plumage in peacocks is not such a drag. *J. Exp. Biol.* **217**, 3237–3241. (doi:10.1242/jeb.107474)
6. Evans MR, Thomas ALR. 1992 The aerodynamic and mechanical effects of elongated tails in the scarlet-tufted malachite sunbird: measuring the cost of a handicap. *Anim. Behav.* **43**, 337–347. (doi:10.1016/S0003-3472(05)80229-5)
7. Oufiero CE, Garland T. 2007 Evaluating performance costs of sexually selected traits. *Funct. Ecol.* **21**, 676–689. (doi:10.1111/j.1365-2435.2007.01259.x)
8. Allen BJ, Levinton JS. 2007 Costs of bearing a sexually selected ornamental weapon in a fiddler crab. *Funct. Ecol.* **21**, 154–161. (doi:10.1111/j.1365-2435.2006.01219.x)
9. Doake S, Scantlebury M, Elwood RW. 2010 The costs of bearing arms and armour in the hermit crab *Pagurus bernhardus*. *Anim. Behav.* **80**, 637–642. (doi:10.1016/j.anbehav.2010.06.023)
10. Goyens J, Dirckx J, Aerts P. 2015 Costly sexual dimorphism in *Cyclommatus metallifer* stag beetles. *Funct. Ecol.* **29**, 35–43. (doi:10.1111/1365-2435.12294)
11. Goyens J, Dirckx J, Dierick M, Van Hoorebeke L, Aerts P. 2014 Biomechanical determinants of bite force dimorphism in *Cyclommatus metallifer* stag beetles. *J. Exp. Biol.* **217**, 1065–1071. (doi:10.1242/jeb.091744)
12. Rink M, Sinsch U. 2007 Radio-telemetric monitoring of dispersing stag beetles: implications for conservation. *J. Zool.* **272**, 235–243. (doi:10.1111/j.1469-7998.2006.00282.x)
13. Frantsevich L. 2011 Mechanisms modeling the double rotation of the elytra in beetles (Coleoptera). *J. Bionic Eng.* **8**, 395–405. (doi:10.1016/S1672-6529(11)60045-0)
14. Frantsevich L. 2012 Double rotation of the opening (closing) elytra in beetles (Coleoptera). *J. Insect Physiol.* **58**, 24–34. (doi:10.1016/j.jinsphys.2011.09.010)
15. Taylor GK, Thomas ALR. 2003 Dynamic flight stability in the desert locust Schistocerca gregaria. *J. Exp. Biol.* **206**, 2803–2829. (doi:10.1242/jeb.00501)
16. Sun M, Xiong Y. 2005 Dynamic flight stability of a hovering bumblebee. *J. Exp. Biol.* **208**, 447–459. (doi:10.1242/jeb.01407)
17. Liang B, Sun M. 2013 Aerodynamic interactions between wing and body of a model insect in forward flight and maneuvers. *J. Bionic Eng.* **10**, 19–27. (doi:10.1016/S1672-6529(13)60195-X)
18. Cimbala JM, Cengel Y. 2008 *Essentials of fluid mechanics: fundamentals and applications*. New York, NY: McGraw-Hill.
19. Menter FR. 1994 Two-equation eddy-viscosity turbulence models for engineering applications. *AIAA J.* **32**, 1598–1605. (doi:10.2514/3.12149)
20. Hoerner SF. 1965 *Fluid dynamic drag: practical information on aerodynamic drag and hydrodynamic resistance*. Bakersfield, CA: Hoerner Fluid Dynamics.
21. Van Wassenbergh S, Van Manen K, Marcroft TA, Alfaro ME, Stamhuis EJ. 2015 Boxfish swimming paradox resolved: forces by the flow of water around the body promote manoeuvrability. *J. R. Soc. Interface* **12**, 20141146. (doi:10.1098/rsif.2014.1146)
22. Hosoya T, Araya K. 2005 Phylogeny of Japanese stag beetles (Coleoptera: Lucanidae) inferred from 16S mtrRNA gene sequences, with reference to the evolution of sexual dimorphism of mandibles. *Zool. Sci.* **22**, 1305–1318. (doi:10.2108/zsj.22.1305)
23. Gotoh H, Cornette R, Koshikawa S, Okada Y, Lavine LC, Emlen DJ, Miura T. 2011 Juvenile hormone regulates extreme mandible growth in male stag beetles. *PLoS ONE* **6**, e211139. (doi:10.1371/journal.pone.0021139)
24. Clark CJ, Dudley R. 2009 Flight costs of long, sexually selected tails in hummingbirds. *Proc. R. Soc. B* **276**, 2109–2015. (doi:10.1098/rspb.2009.0090)
25. Ribak G, Swallow JG. 2007 Free flight maneuvers of stalk-eyed flies: do eye-stalks affect aerial turning behavior? *J. Comp. Physiol. A* **193**, 1065–1079. (doi:10.1007/s00359-007-0259-1)
26. Goyens J, Soons J, Aerts P, Dirckx J. 2014 Finite element modelling reveals force modulation of jaw adductors in stag beetles. *J. R. Soc. Interface* **11**, 20140908. (doi:10.1098/rsif.2014.0908)
27. Tatsuta H, Mizota K, Akimoto S. 2001 Allometric patterns of heads and genitalia in the stag beetle *Lucanus maculifemoratus* (Coleoptera: Lucanidae). *Ann. Entomol. Soc. Am.* **94**, 462–466. (doi:10.1603/0013-8746(2001)094[0462:APOHAG]2.0.CO;2)
28. Kawano K. 2006 Sexual dimorphism and the making of oversized male characters in beetles (Coleoptera). *Ann. Biomed. Eng.* **99**, 327–341. (doi:10.1603/0013-8746(2006)099)
29. Kawano K. 2000 Genera and allometry in the stag beetle family Lucanidae, Coleoptera. *Ann. Entomol. Soc. Am.* **93**, 198–207. (doi:10.1603/0013-8746(2000)093)
30. McCullough EL, Emlen DJ. 2013 Evaluating the costs of a sexually selected weapon: big horns at a small price. *Anim. Behav.* **86**, 977–985. (doi:10.1016/j.anbehav.2013.08.017)